

Direct dehydrogenation of methanol to anhydrous formaldehyde over $\text{Ag}_2\text{O}/\gamma\text{-Al}_2\text{O}_3$ nanocatalysts at relatively low temperature

Abd El-Aziz A. Said¹ · Mohamed Abd El-Aal¹

Received: 16 August 2016 / Accepted: 25 November 2016
© Springer Science+Business Media Dordrecht 2016

Abstract A series of $\text{Ag}_2\text{O}/\gamma\text{-Al}_2\text{O}_3$ nanocatalysts for direct dehydrogenation of methanol with various extents of Ag_2O loading (0.5–15 wt%) were prepared by the wet impregnation method. The catalysts were characterized by XRD, TEM and N_2 sorption. The catalysts were tested for direct dehydrogenation of methanol in a fixed-bed reactor at a relatively low temperature, 330 °C, using N_2 as a carrier gas. The obtained results revealed that pure $\gamma\text{-Al}_2\text{O}_3$ exhibits quite poor selectivity toward formaldehyde (FA) formation ($\approx 28\%$). On the other hand, the addition of Ag_2O improves the catalytic activity of $\gamma\text{-Al}_2\text{O}_3$ where the catalyst with 10 wt% Ag_2O exhibits 100% conversion of methanol with 100% yield of FA. Moreover, the catalyst with 1 wt% Ag_2O achieved similar results at the reaction temperature of 370 °C.

Keywords $\text{Ag}_2\text{O}/\gamma\text{-Al}_2\text{O}_3$ · Methanol · Dehydrogenation · Anhydrous formaldehyde

Introduction

Formaldehyde (FA) has received wide attention due to its important applications in many fields, such as the production of raw material for other chemical products, including the production of new plastics, phenol or urea formaldehyde resin. In addition, it can be used in synthetic polymer materials, new drug intermediates, advanced perfumes and dyes [1]. Generally, anhydrous FA in industry is obtained by the dehydration reaction of an aqueous solution of FA, which is mainly produced from the partial oxidation of methanol by air in the presence of a silver catalyst or a Fe-Mo catalyst [2, 3]. However, FA forms an azeotrope with water, making the

✉ Abd El-Aziz A. Said
aasaid55@yahoo.com

¹ Chemistry Department, Faculty of Science, Assiut University, Assiut 71516, Egypt

removal of water and methanol from the aqueous solution of FA is very expensive. Thus, the direct dehydrogenation of methanol to anhydrous FA is a desirable route because it is able to avoid the disadvantages of oxidation and separation problems (FA and H_2 can be easily separated).

Methanol can be converted to anhydrous FA and hydrogen without any catalyst at a very high temperature, 900 °C, with the FA yield being less than 20%, and with only 43% selectivity toward FA [4]. Yunan [5] studied the direct dehydrogenation of methanol to anhydrous FA over a $Li_{0.5}Na_{0.5}AlO_2$ catalyst. He found that the maximum yield of FA was 70% at the reaction temperature of 900 °C. Consequently, the challenge is to manage the direct dehydrogenation of methanol to anhydrous FA at a lower temperature over highly active and selective catalysts.

Ren et al. [6] reported the results of the direct dehydrogenation of methanol to anhydrous FA over polycrystalline silver, Ag–SiO₂–MgO [7], Ag–SiO₂–Al₂O₃ [8], Ag–SiO₂–Al₂O₃–ZnO [9], and Ag–SiO₂–MgO–Al₂O₃ [3] catalysts. They observed that the polycrystalline silver after pre-treatment with oxygen at high temperature showed excellent activity and selectivity at 600 °C. It exhibited 100% of both methanol conversion and selectivity toward anhydrous FA. They also found that the Ag–SiO₂–MgO catalyst exhibited activity of 96% conversion and 75% yield of FA under the optimum conditions of 20 wt% loading of silver and 650 °C reaction temperature. On the other hand, the Ag–SiO₂–Al₂O₃ catalyst showed a catalytic performance of 95% methanol conversion and 81.2% of FA yield using 18 wt% loading of silver and 650 °C. In addition, the Ag–SiO₂–Al₂O₃–ZnO catalyst showed a catalytic activity of 99% conversion and 87% selectivity under optimum conditions (20 wt% loading of silver, zinc content 15% and 650 °C). Moreover, they observed that the Ag–SiO₂–MgO–Al₂O₃ catalyst with mass ratios of 20:55.2:8.3:16.5 for Ag, SiO₂, MgO and Al₂O₃, respectively, showed a highly efficient catalytic performance with 100% conversion and 100% selectivity toward FA formation. Unfortunately, the operating temperature (650 °C) and the percentage of Ag (20 wt%) are both very high. According to the previous survey, the development of a new catalytic system able to convert methanol to anhydrous FA at a relatively low temperature using low-cost materials is in great demand. However, the direct dehydrogenation of methanol over a Ag₂O/ γ -Al₂O₃ catalyst to anhydrous FA has not, to the best of our knowledge, been reported yet. Hence, our present work is to report a series of Ag₂O/ γ -Al₂O₃ catalysts prepared by the impregnation method that show significantly high catalytic performance in the direct dehydrogenation of methanol to anhydrous FA. X-ray diffraction, BET and transmission electron microscopy (TEM) have been used for their characterization.

Experimental

Catalyst preparation

Aluminum nitrate nonahydrate $Al(NO_3)_3 \cdot 9H_2O$ (Oxford Assay 98.5%), silver nitrate $AgNO_3$ (Sigma Aldrich), ammonia solution (NH_4OH 23%) and methyl alcohol were obtained as pure reagents and used without further purification. The

preparation of γ -Al₂O₃ has been described in our previous work [10]. For the aluminum nitrate precursor, after precipitation by ammonia solution at pH = 7, the resulting precipitate was filtered and washed by bi-distilled water several times. The precipitate was dried at 100 °C for 24 h and calcined at 500 °C in a static air atmosphere for 3 h. The Ag₂O/ γ -Al₂O₃ catalysts with different loadings of Ag₂O (0.5–15 wt%) were prepared by a wet impregnation method and designed as 0.5–15% SA. The typical synthesis procedure was illustrated by 10% SA. An amount of 0.2932 g of silver nitrate was dissolved in small amounts of bi-distilled water, and then 1.8 g of the prepared γ -Al₂O₃ powder was added and the mixture was admixed carefully to obtain a homogeneous paste. The mixture produced was dried at 100 °C for 24 h before being calcinated at 500 °C in a static air atmosphere for 3 h.

Catalyst characterization

Powder X-ray diffraction (XRD) experiments of the catalysts were performed using a Philips (The Netherlands) diffractometer (Model PW 2103, $\lambda = 1.5418 \text{ \AA}$, 35 kV and 20 mA) with a source of CuK α radiation (Ni filtered). Particle size was estimated using Scherrer's formula [11].

TEM with a high-resolution experimental microscope (Tecnai G2-model Spirit Twin-120 KV) was used to investigate the size and the morphology of the catalysts. The catalyst powder was dispersed in ethanol using ultrasonic radiation for 20 min and a drop of that suspension was placed onto the carbon-coated grids. The degree of magnification of the TEM images was the same for all the investigated catalysts. Average particle size and particle size distribution were obtained manually by measuring the diameter of the possible number of particles from the TEM image. The mean particle diameter (d_M) was calculated as in the previous report [12] by the formula:

$$d_M = \sqrt{\frac{(\sum n_i \times d_i^2)}{\sum n_i}}$$

where d_i is the particle size and n_i is the number of particles in the size range between $d_i + \Delta$ and $d_i - \Delta$.

Brunauer–Emmett–Teller (BET) analysis was performed using a Nova 3200 (Quantachrom Instruments, USA). The surface areas and pore volumes were measured by N₂ adsorption and the desorption isotherm was $-196 \text{ }^\circ\text{C}$.

Catalytic evaluation test

The catalytic dehydrogenation of methyl alcohol was performed to evaluate the efficiency of the prepared materials as catalysts. The catalytic run was carried out at 330 °C in a conventional fixed-bed flow-type reactor at atmospheric pressure using nitrogen as a carrier gas. The measurement procedure was similar to that reported previously [13]. Each catalytic run was conducted using 500 mg of the powdered catalyst and the total flow rate was fixed at 50 ml min⁻¹ and 4% methanol in the gas

feed. The products were analyzed by on-line gas chromatography using a 2-m DNP glass column. Measurements of the conversion and yield (%) were recorded after 1 h from the initial introduction of the reactant into the reactor to ensure the attainment of the reaction equilibrium (steady-state conditions). Methanol conversion (C), FA selectivity (S) and yield of FA (Y) were used to assess the activity of the catalysts [14].

$$C(\%) = \frac{[\text{Methanol}]_{\text{in}} - [\text{Methanol}]_{\text{out}}}{[\text{Methanol}]_{\text{in}}} \times 100$$

$$S(\%) = \frac{[\text{FA}]}{[\text{FA}] + [\text{by-products}]} \times 100$$

$$Y(\%) = \frac{(C \times S)}{100}$$

In these equations, $[\text{Methanol}]_{\text{in}}$ and $[\text{Methanol}]_{\text{out}}$ denote the peak areas (concentrations) of methanol at the reactor inlet and outlet, respectively.

Results and discussion

Catalyst characterization

The XRD patterns of $\gamma\text{-Al}_2\text{O}_3$, 1, 10 and 15% SA (fresh and used) catalysts are shown in Fig. 1. For 1, 10 and 15% SA fresh samples, the presence of typical γ phase Al_2O_3 diffraction peaks at $2\theta = 46^\circ$ and 66.5° were observed [15]. This result indicates that the addition of silver oxide to $\gamma\text{-Al}_2\text{O}_3$ did not affect the polymorphs of the alumina support [16], and an increase in the Ag_2O content was found to be accompanied by a decrease in the intensities of the XRD peaks associated with the $\gamma\text{-Al}_2\text{O}_3$ phase. In addition, diffraction peaks of Ag_2O at $2\theta = 32.4^\circ$, 37.6° , 54.2° and 64.6° (JCPDS file 04-005-4923), and low intensity diffraction peaks corresponding to metallic silver at $2\theta = 44.1^\circ$ and 77° (JCPDS file 04-002-1347) were also detected. It is known that silver can be easily reduced to a metallic state at temperatures higher than 300°C [17]. Thus, 10 and 15% SA fresh samples showed low-intensity diffraction peaks corresponding to metallic Ag. After the direct dehydrogenation reaction of methanol, there was a new sharp peak appeared at $2\theta = 37.9^\circ$, which can be ascribed to the crystalline Ag. Also, an observable increase in the intensities of the diffraction peaks at $2\theta = 44.1^\circ$ and 77° . This behavior can be explained as the silver ion (Ag^{2+}) in the fresh samples can be reduced to the metallic state Ag by H_2 released during the dehydrogenation reaction. It can also observe that there are still diffraction peaks corresponding to Ag_2O in the used samples. The absence of the diffraction peaks due to Ag-species in 1% SA fresh sample may be due to the small amounts of silver oxide added were below the detection limits of the X-ray diffractometer used [18]. The diffraction peaks at $2\theta = 46^\circ$ and 66.5° for $\gamma\text{-Al}_2\text{O}_3$ phase, at $2\theta = 32.4^\circ$, 37.6° , 54.2° , and 64.6° for the Ag_2O phase and at $2\theta = 37.9^\circ$, 44.1° , and 77° for the Ag phase were selected

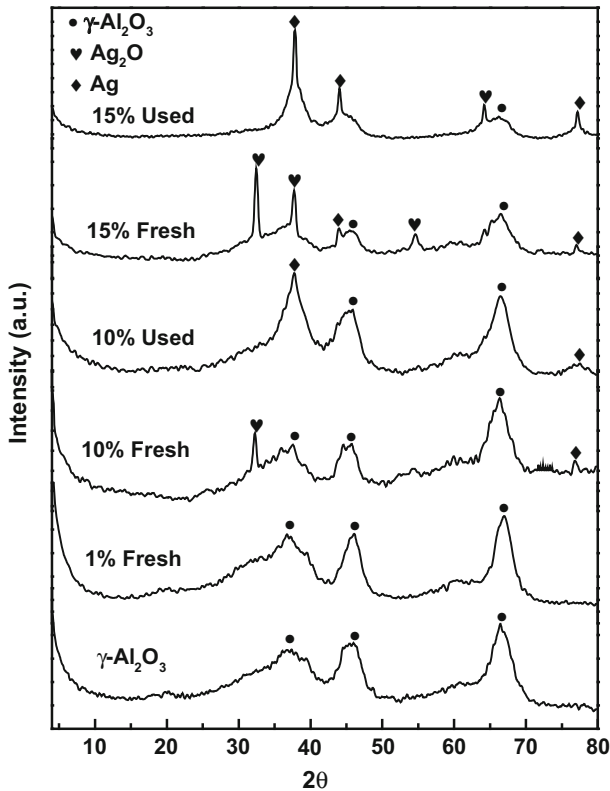


Fig. 1 X-ray diffractograms of pure γ - Al_2O_3 , 1, 10 and 15% SA catalysts (fresh and used)

for calculating the crystallites sizes. The averages of these calculations were reported as the crystallite sizes for each phase are cited in Table 1. It was observed that the crystallite size of γ - Al_2O_3 did not change with the addition of Ag_2O after or before the reaction. Moreover, the crystallite sizes for Ag_2O and Ag phases slightly increase with increasing silver oxide loading.

Table 1 The crystallite (D) and mean particle (d_M) sizes for γ - Al_2O_3 , 1, 10 and 15% SA (fresh and used) samples calcined at 500 °C

Sample	$D_{\text{Al}_2\text{O}_3}$ (nm)	$D_{\text{Ag}_2\text{O}}$ (nm)	D_{Ag} (nm)	d_M (nm)
γ - Al_2O_3	8	–	–	–
1% SA (fresh)	11	–	–	6.3 ± 3.1
10% SA (fresh)	12	22	12	9.2 ± 3.1
10% SA (used)	12	–	18	–
15% SA (fresh)	–	19	29	9.2 ± 2.9
15% SA (used)	–	35	30	12 ± 4.5

TEM was used to determine the morphology of the catalysts before and after the methanol dehydrogenation reaction and the silver species particle size distribution. TEM images of γ -Al₂O₃, 10% SA and 15% SA (fresh and used) catalysts as well as the Ag₂O and Ag⁰ nanoparticles size distribution are presented in Fig. 2. These pictures show that γ -Al₂O₃ support appears as small aggregates with average particle size of about 8–14 nm. On the other hand, the catalysts (1, 10 and 15% SA) presented the spherical Ag₂O particles, well distributed on the support.

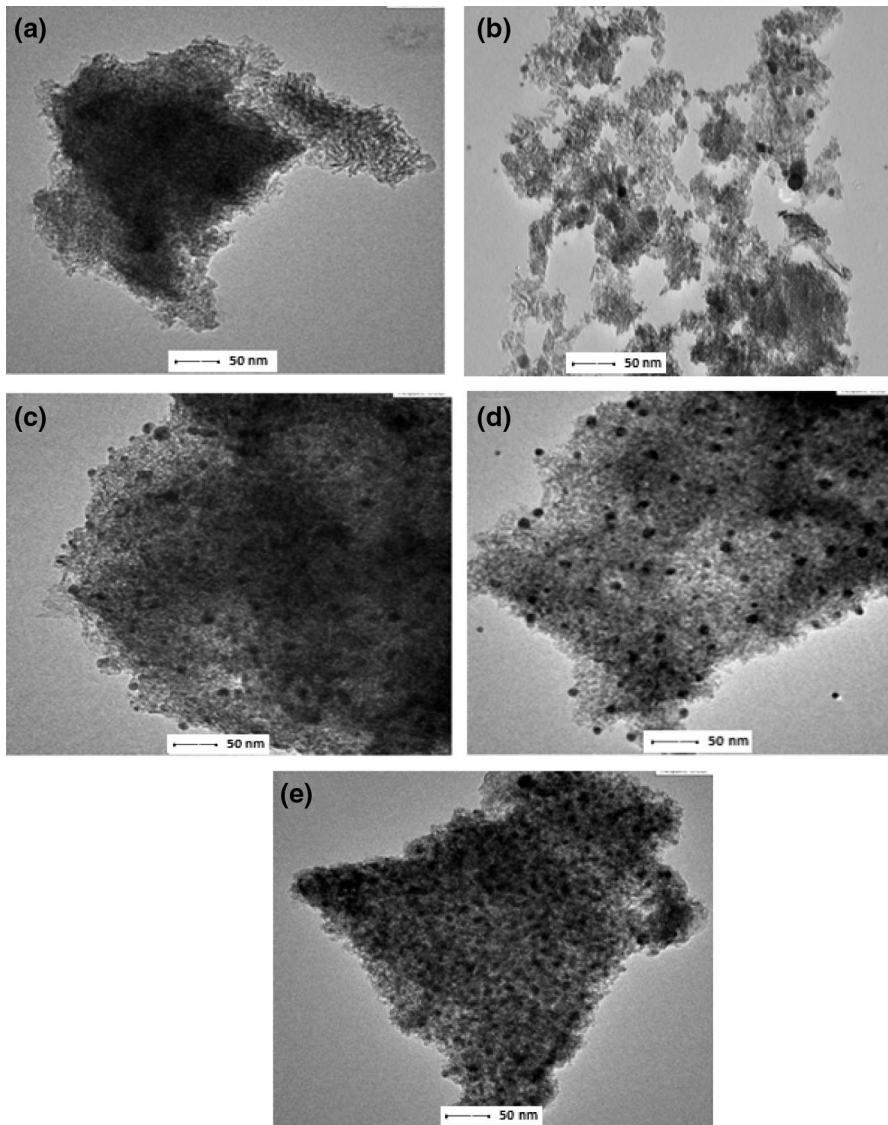


Fig. 2 TEM Images of **a** γ -Al₂O₃, **b** 1% SA fresh, **c** 10% SA fresh, **d** 15% SA fresh and **e** 15% SA used and the particle size distribution

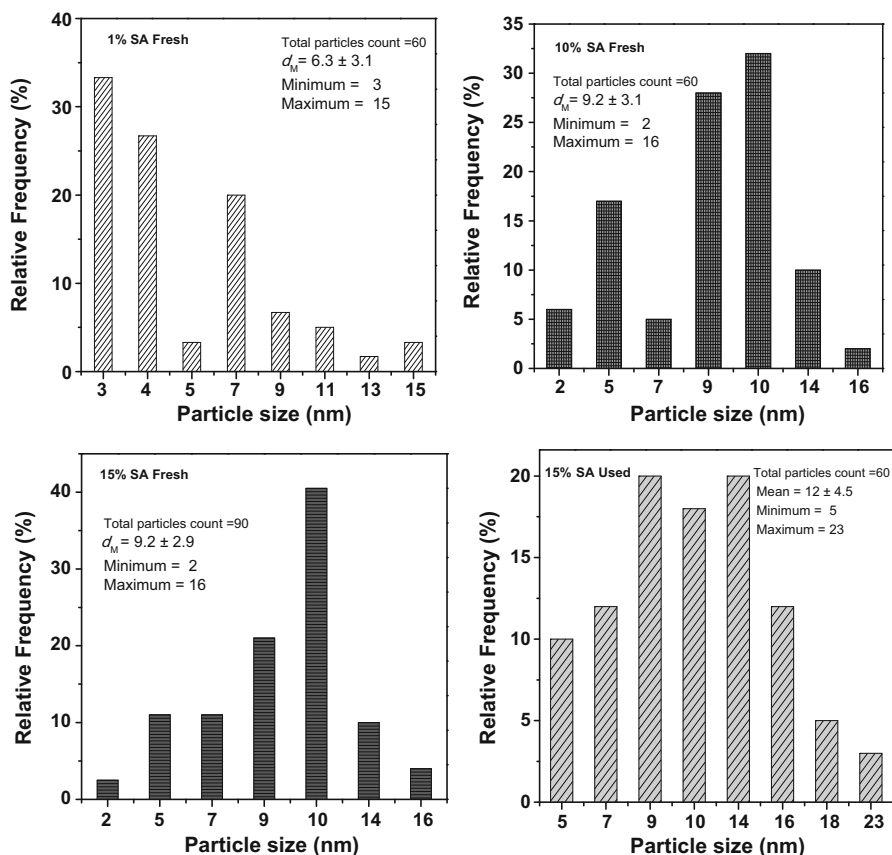


Fig. 2 continued

Measurements of the size distribution based on the images showed a mean particle size of 6.3 ± 3.1 for 1% SA fresh sample with a narrow distribution range of 3–15 nm. On the other hand, the mean particle size and the distribution ranges of the 10 and 15% SA fresh samples are 9.2 nm and 2–16 nm, respectively. As can be seen, some small Ag_2O particles aggregated into larger ones and the others reduced to metallic Ag after the reaction test [19] (Fig. 2d); the largest particle was about 23 nm in diameter. The mean particle sizes of the samples are cited in Table 1. The results indicate that increasing the Ag_2O content slightly increases the mean particle size. On the other hand, the mean particle size increases after the reaction. It is worth mentioning here that the crystallite size estimated from the XRD peak width is larger than the particle size measured by TEM [20, 21]. This behavior can be explained on the basis of the samples with nanoparticles polydispersed in size, the Scherrer equation applied to XRD data gives an indication of the size of only the largest present particles [22].

The nitrogen adsorption–desorption isotherms (a) and the corresponding BJH pore size distribution (b) of $\gamma\text{-Al}_2\text{O}_3$, 1, 10 and 15% SA catalysts are represented in

Fig. 3. All isotherms are of type IV, which is a characteristic feature of mesoporous materials with H2 hysteresis loops. The pore size distribution calculated from desorption branch is shown in Fig. 3b. This shows that the pore diameters were ≈ 4.9 nm and slightly changed with the surface modifications with Ag_2O loadings. The observed changes of specific surface area (S_{BET}) and pore volume as well as

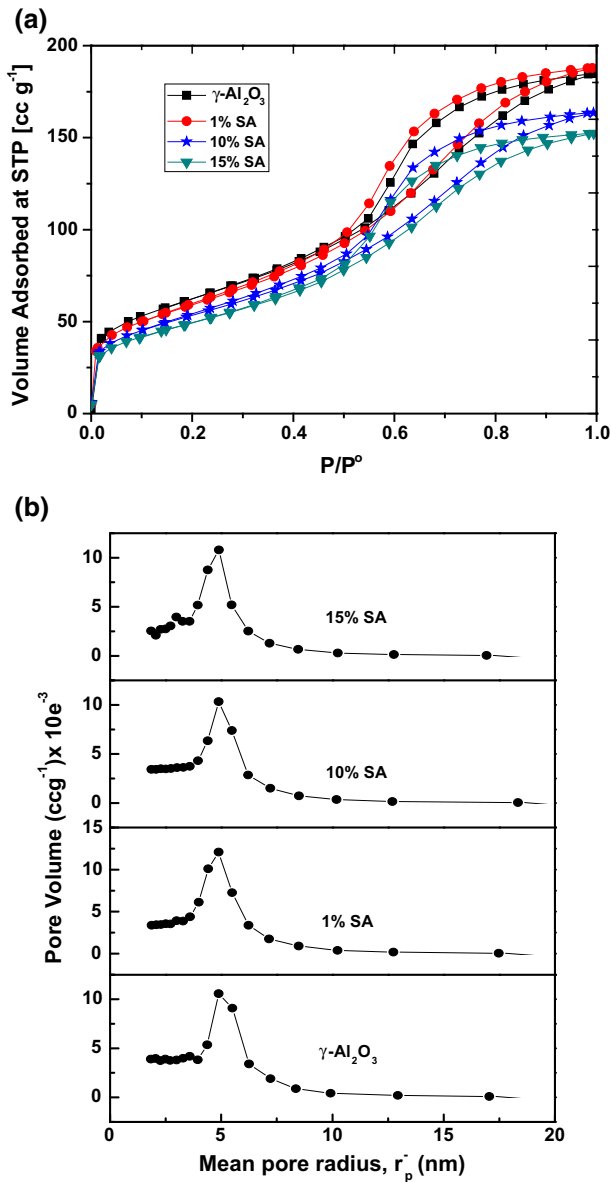


Fig. 3 a Nitrogen adsorption–desorption isotherms of pure $\gamma\text{-Al}_2\text{O}_3$, 1, 10 and 15% SA catalysts. b Pore size distribution of pure $\gamma\text{-Al}_2\text{O}_3$, 1, 10 and 15% SA catalysts

pore size are shown in Table 2. The surface area and pore volume decrease as a result of the incorporation of Ag₂O nanoparticles into the mesoporous channels of the support [23].

Catalytic dehydrogenation of methanol to anhydrous FA

The effect of loading γ -Al₂O₃ with different percentages of Ag₂O (0.5–15 wt%) on the direct dehydrogenation of methanol to anhydrous FA was investigated at 330 °C and is illustrated in Fig. 4. Under our operating conditions, pure γ -Al₂O₃ by itself exhibits high conversion of methanol \approx 90%, with 72 and 28% selectivity toward DME and FA formation, respectively. The additions of Ag₂O to γ -Al₂O₃ lead to an observable increase in the conversion and selectivity toward FA. In addition, the 10% SA sample shows the maximum activity of 100% conversion and 100% yield of FA. As compared with our results and those previously published in the literature, from an economical point of view, the 10% SA catalyst is the best one because it gives outstanding activity using a low temperature and low percentage of Ag₂O.

The most important parameters affecting the direct dehydrogenation of methanol to anhydrous FA are the reaction temperature, % methanol, reaction time and catalyst calcination temperature. We choose the 1% SA catalyst for studying different parameters because we have tried to reduce the percentage loading of Ag₂O. This, the effect of reaction temperature on the direct dehydrogenation of methanol over the 1% SA catalyst was studied and is shown in Fig. 5. This figure demonstrates that the reaction starts at 125 °C with 3% conversion and 100% selectivity toward DME. On increasing the reaction temperature up to 250 °C, it shows a promising activity of \approx 92.4% of methanol conversion with a remarkable yield of DME. Thus, the 1% SA catalyst can be used as an efficient catalyst for methanol dehydration to DME at that temperature. On the other hand, with increasing the reaction temperature above 250 °C, the selectivity toward DME decreases whereas the selectivity toward FA increases. At 370 °C, the 1% SA catalyst exhibits the best activity with 100% conversion and 100% selectivity

Table 2 Variation of specific surface area and pore characteristics of Ag₂O/ γ -Al₂O₃ catalysts calcined at 500 °C

Wt% Ag ₂ O	S_{BET} (m ² g ⁻¹)	S_t (m ² g ⁻¹)	C_{BET}	Total pore volume (cc g ⁻¹)	Average pore diameter (nm)
γ -Al ₂ O ₃	222	222	130	0.284	5.1
0.5	221	221	143	0.277	5.5
1	211	211	143	0.275	5.5
3	204	204	152	0.270	5.3
5	203	203	162	0.267	5.4
7	201	201	140	0.265	5.4
10	190	190	153	0.252	5.3
15	176	176	153	0.235	5.3

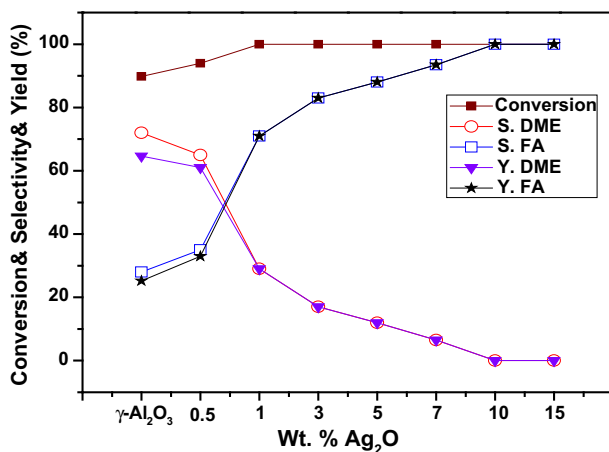


Fig. 4 Catalytic dehydrogenation of methanol over pure γ -Al₂O₃ and 0.5–15% SA catalysts at 330 °C

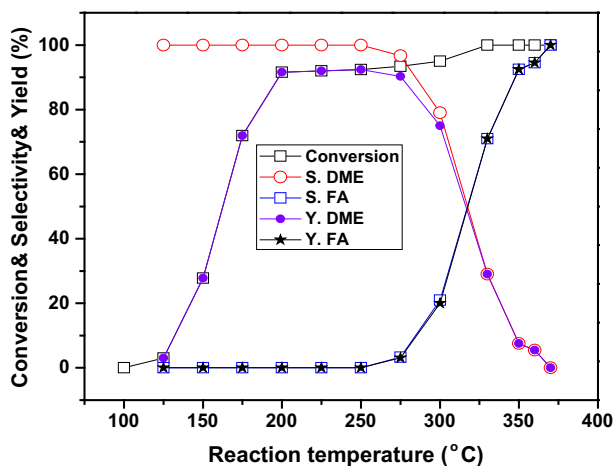


Fig. 5 Effect of reaction temperature on the dehydrogenation–dehydration of methanol over the 1% SA catalyst calcined at 500 °C

toward FA formation. From the above results, it is clear that the 1% SA catalyst has a dual function because at 250 °C can be used as an efficient catalyst in DME production while it can be also be applied as an outstanding catalyst in the synthesis of anhydrous FA at 370 °C.

The effect of % methanol on the activity of the 1% SA catalyst at 370 °C was investigated and the results are presented in Fig. 6, showing that the higher activity toward the FA formation (100% yield) was obtained when using 4% of methanol. Moreover, an increase in the % of methanol led to an observable decrease in methanol conversion and the yield of FA, and at the same time the yield of DME increases. For example, when using 19.5% of methanol, the 1% SA catalyst exhibits

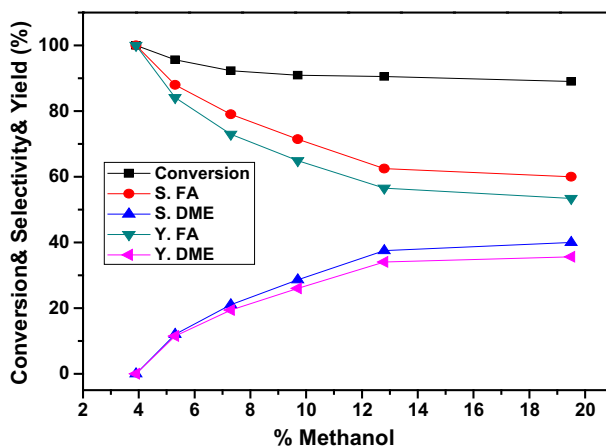


Fig. 6 Effect of % methanol on its dehydrogenation–dehydration over 1% SA catalyst calcined at 500 °C

89% of methanol conversion, with 53.4 and 35.6% yield of FA and DME, respectively.

The effect of calcination temperature on the catalytic activity of the 1% SA catalyst toward methanol dehydrogenation to anhydrous FA at 370 °C was studied on the catalyst calcined at 500, 550, 650 and 750 °C and the results are illustrated in Fig. 7, showing that raising the calcination temperature does not affect on the catalytic activity of the catalyst. These results reflect that the active sites responsible for the direct methanol dehydrogenation unchanged with increasing the calcination temperature up to 750 °C and this provides another excellent value added to the novel behavior of our catalyst.

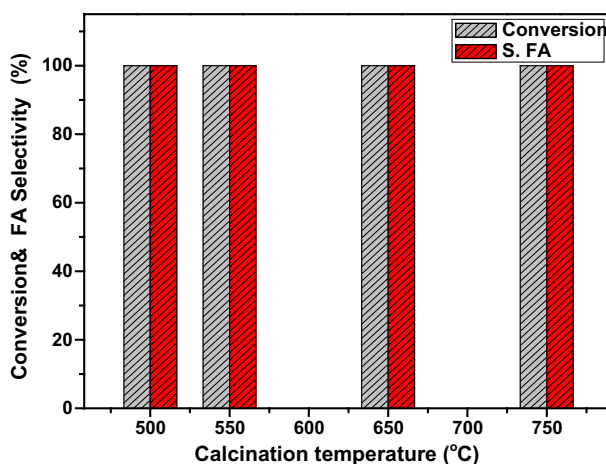


Fig. 7 Effect of catalyst calcination temperature on methanol dehydrogenation over the 1% SA catalyst at 370 °C

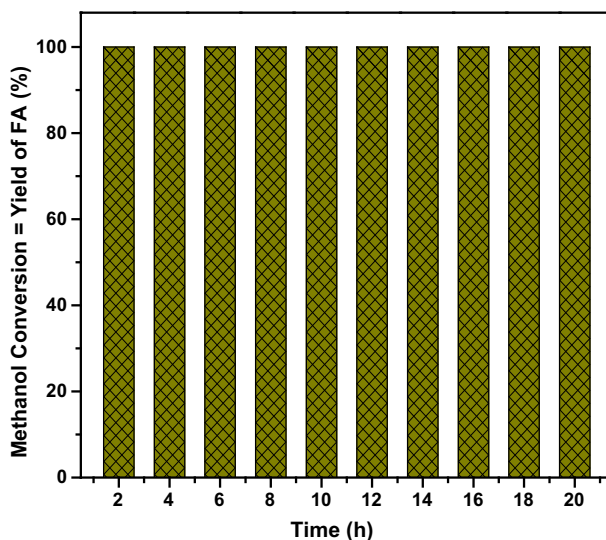


Fig. 8 Effect of reaction time on the catalytic dehydrogenation of methanol over the 1% SA catalyst calcined at 500 °C

Stability of the catalyst

It was accepted that the most important feature of the catalyst is the stability during the reaction for a long lifetime. So, the long-term stability of 1% SA calcined at 500 °C was carried out at 370 °C reaction temperature and using 4% methanol. The obtained results are presented in Fig. 8. It shows that the methanol conversion and the yield of FA remained constant for 20 h, which indicated that no noticeable deactivation of the catalyst was occurred. However, it was reported that Ag–SiO₂–Al₂O₃–ZnO catalyst showed a much longer lifetime (about 2 h) than the Ag–SiO₂–Al₂O₃ and Ag–SiO₂–ZnO catalysts (only 1 h) [9]. So, in comparison with our results with previously published data we found that our catalyst is the most stable one in direct dehydrogenation of methanol to anhydrous FA.

Conclusions

In this work, nano-Ag₂O/γ-Al₂O₃ catalyst prepared by a simple conventional impregnation method is demonstrated to be an outstanding efficient catalyst for the direct dehydrogenation of methanol to anhydrous FA. Detailed structural analysis by XRD, TEM and BET methods showed that the catalyst is mesoporous in nature and, during the direct dehydrogenation reaction, Ag₂O is reduced to metallic Ag with a slight increase in particle size being observed. The catalytic performance of the catalyst is mainly dependant on the content of Ag₂O and the reaction temperature. The catalyst with 10 wt% Ag₂O loading exhibits excellent catalytic activity, with selectivity to anhydrous FA reaching 100% with a methanol conversion of 100% at relatively low temperature of 330 °C. Moreover, the catalyst

with 1 wt% Ag₂O gives 100% yield of anhydrous FA at 370 °C, and no appreciable deactivation is observed even after reacting for more than 20 h.

References

1. Y. Sheng, Y. Wang, W. Zhizhong, S. Jun, Method for preparing anhydrous formaldehyde industrial catalyst by methanol dehydrogenation, Patent No CN101147872A (2008)
2. S. Ruf, A. May, G. Emig, Appl. Catal. A Gen. **213**, 203 (2001)
3. L.-P. Ren, W.-L. Dai, Y. Cao, H. Li, K. Fan, Chem. Commun. **24**, 3030 (2003)
4. H.-J. Li, A.C. Lausche, A.A. Peterson, H.A. Hansen, F. Studt, T. Bligaard, Surf. Sci. **641**, 105 (2015)
5. Q. Yunan, China Molybd. Ind. **6**, 21 (2001)
6. L.-P. Ren, W.-L. Dai, X.-L. Yang, J.-H. Xu, Y. Cao, H. Li, K. Fan, Catal. Lett. **99**, 83 (2005)
7. L.-P. Ren, W.-L. Dai, Y. Cao, K.-N. Fan, Catal. Lett. **85**, 81 (2003)
8. L.-P. Ren, W.-L. Dai, Y. Cao, H.-X. Li, W.-H. Zhang, K.-N. Fan, Acta Chem Sincia **61**, 937 (2003)
9. L.-P. Ren, W.-L. Dai, X.-L. Yang, Y. Cao, H. Li, K.-N. Fan, Appl. Catal. A Gen. **273**, 83 (2004)
10. A.A. Said, M.M.M.A. El-Wahab, M.A. El-Aal, Monatsh Chem. **147**, 1507 (2016)
11. B.D. Cullity, *Elements of x-ray Diffraction*, 3rd edn. (Addison-Wesley, Reading, 1967)
12. J. Peng, S. Wang, Appl. Catal. B Gen. **73**, 282 (2007)
13. A.A. Said, M.M.A. El-Wahab, M.A. El-Aal, J. Mol. Catal. A Chem. **394**, 40 (2014)
14. A.A. Said, M.M.M.A. El-Wahab, A.M. Alian, Catal. Lett. **146**(1), 82 (2016)
15. A.A. Said, M.M.M.A. El-Wahab, M.A. El-Aal, Res. Chem. Intermedia. **42**, 1537 (2016)
16. L. Yu, Q. Zhong, S. Zhanga, Phys. Chem. Chem. Phys. **16**, 12560 (2014)
17. W.-L. Dai, Y. Cao, L.-P. Ren, X.-L. Yang, J.-H. Xu, H.-X. Li, H.-Y. He, K.-N. Fan, J. Catal. **228**, 80 (2004)
18. G.A. El-Shobaky, M.A. Shouman, S.M. El-Khouly, Mater. Lett. **58**, 184 (2004)
19. L. Zhang, C. Zhang, H. He, J. Catal. **261**, 101 (2009)
20. N. Toshima, H. Yan, Y. Shiraiishi, Metal Nanoclusters in Catalysis and Materials Science: The Issue of Size Control, Chap. 3, ed. by B. Corain, G. Schmid, N. Toshima (Elsevier, Netherlands, 2008), p. 62.
21. S.E. Lin, K. Borgohain, W.C.J. Wei, J. Am. Ceram. Soc. **89**(12), 3266 (2006)
22. R. Wojcieszak, M.J. Genet, P. Eloy, P. Ruiz, E.M. Gaigneaux, J. Phys. Chem. C **114**, 16677 (2010)
23. G. Zhan, J. Huang, M. Du, D. Sun, I. Abdul-Rauf, W. Lin, Y. Hong, Q. Li, Chem. Eng. J. **187**, 232 (2012)